Potential Energy Surfaces for Gas-Phase S_N2 Reactions Involving Nitriles and Substituted Nitriles

Travis D. Fridgen,*,† Jami L. Burkell,‡,§ Ashraf N. Wilsily,‡ Vicki Braun,‡ Josh Wasylycia,‡ and Terry B. McMahon‡,§

Department of Chemistry, Memorial University of Newfoundland, St. John's, NL A1C 5S7, Department of Chemistry, University of Waterloo, Waterloo, Ontario, Canada N2L 3G1, and Guelph-Waterloo Centre for Graduate Work in Chemistry, University of Waterloo, Waterloo, Ontario, Canada N2L 3G1

Received: February 4, 2005; In Final Form: June 27, 2005

The stationary points on the potential energy surfaces for a number of gas-phase S_N2 reactions have been determined using a combination of pulsed ionization high-pressure mass spectrometry. MP2/6-311++G**//B3LYP/6-311+G** calculations are shown to provide excellent agreement with the experimentally determined values, providing confidence for the use of this computational method to predict values that are not available experimentally. The binding in the halide/nitrile complexes has been described in the past as either hydrogen bonding or electrostatic bonding. The trends in the binding energies observed here, though, cannot be rationalized in terms of simply hydrogen bonding or ion−dipole bonding but a mixture of the two. The computed structures support the description of binding as a mixture of hydrogen bonding and ion−dipole bonding.

1. Introduction

Gas-phase bimolecular nucleophilic displacement (S_N2) reactions have been the focus of many studies[1] with the aim to determine quantitatively detailed potential energy surfaces for various nucleophile/substrate pairs. Solution−phase S_N2 reactions are one of the most widely studied classes of reactions in chemistry and are thoroughly detailed in physical organic chemistry textbooks.[2,3] For a typical solution-phase S_N2 reaction such as that shown in eq 1,

$$X^- + RY \rightarrow Y^- + RX \qquad (1)$$

where X and Y are halogens and R is an alkyl group, the kinetics were recognized to be first order in both the nucleophile (X^-) and substrate (RY), making it a second-order reaction occurring in one elementary step.

The second-order kinetics were believed to be the result of attack on the substrate by the nucleophile, displacing the leaving group in a single reaction step. Experiments showing inversion at the site of substitution imply attack at the backside of the substrate. This reaction was observed to proceed very slowly with a single large energy barrier, as shown in the potential energy profile for the solution-phase reaction in Figure 1a. This rather featureless potential energy surface is adequate to represent and describe the solution-phase reactivity. However, the gas-phase S_N2 reaction has proven to be significantly more complicated and the potential energy profile in Figure 1a is not sufficient to describe it. Therefore, it is desirable to discern the details of the potential energy surface in the absence of solvent and to study the structural and electronic effects determining intrinsic reactivity. As well as being fundamentally quite interesting, results of these gas-phase studies can be compared with solution-phase results and the effect of solvent can be more readily assessed.

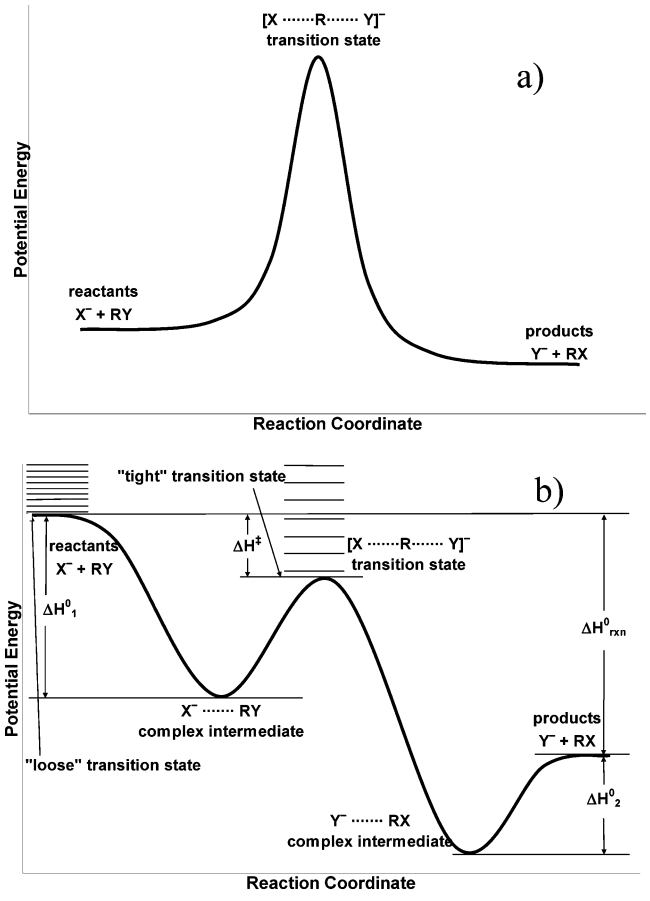

Figure 1. Potential energy surfaces for (a) the solution-phase S_N2 reaction and (b) the gas-phase S_N2 reaction.

Bohme and Brauman pioneered the study of gas-phase S_N2 reactions. In Bohme's group a flowing afterglow system was

* To whom correspondence should be addressed. E-mail: tfridgen@wlu.ca.
† Memorial University of Newfoundland.
‡ Department of Chemistry, University of Waterloo.
§ Guelph-Waterloo Centre for Graduate Work in Chemistry, University of Waterloo.

10.1021/jp058040i CCC: $30.25
Published on Web 07/29/2005

used to determine rate constants for S_N2 reactions[4,5] whereas Brauman and co-workers[6,7] used a pulsed ion cyclotron resonance (ICR) spectrometer. From these experiments it was shown that by changing the nucleophile, leaving group, and alkyl moiety the rate of the reaction also varied dramatically. Olmstead and Brauman examined many different S_N2 reactions and were puzzled by the differing rates of reaction that ranged from almost collision rate to being too slow for the reaction to be observed. The solution-phase potential energy surface clearly could not be applied to the gas-phase reactions because the barrier would prevent the reaction from occurring at the collision rate.

Dougherty et al.[8] had observed stable intermediates corresponding to complexes between various halides and alkyl halide substrates using high-pressure mass spectrometry (HPMS). Binding energies in the range 35−60 kJ mol^{-1} were determined for these complexes. If the stable intermediates were the only feature on the gas-phase S_N2 potential energy surface between reactants and products, then exothermic reactions should occur at close to the collision rate; however, most reactions were found to occur at less than 10% of the collision rate. A single-well potential energy surface also did not provide an adequate picture. Olmstead and Brauman postulated that the potential energy profile for a gas-phase S_N2 reaction actually had a double well potential, as shown in Figure 1b. The variation in the rates of different S_N2 reactions, then, should correlate with the magnitude of the central energy barrier. A complete and detailed explanation of the double well potential and its relation to observables such as the reaction rate is found in refs 1b and 7.

The double well model complicates the mechanism slightly in that the S_N2 reaction can no longer be thought of as a one-step process, as may be the case for the solution-phase reaction. Rather, the reaction can be thought of as occurring in a series of three reversible steps, as outlined in eqs 2−4.

$$X^- + RY \rightleftharpoons X^- \cdots RY \quad (2)$$

$$X^- \cdots RY \rightleftharpoons XR \cdots Y^- \quad (3)$$

$$XR \cdots Y^- \rightleftharpoons RX + Y^- \quad (4)$$

The first step (eq 2) is clustering of the nucleophile and substrate, forming an intermediate represented by the first well. This cluster undergoes a rearrangement that can be thought of as an intramolecular S_N2 reaction (eq 3). This step connects the first intermediate to the second intermediate and is formally an alkyl cation exchange reaction from one halide to another if X^- and Y^- represent halide anions. For an exothermic reaction this process is the rate determining step. The second intermediate then dissociates, forming a new halide and alkyl halide in the third elementary step (eq 4).

In the potential energy profile for a gas-phase S_N2 reaction there are two types of broadly defined transition states, as shown in Figure 1b. The first is a loose, orbiting transition state, and the second is a tight transition state. Even though the central barrier shown here is lower in enthalpy than the orbiting transition state in the entrance channel, taking entropy into account could make the tight transition state higher in free energy, resulting in a free-energy barrier to exchange. From a statistical point of view, the density of states for the orbiting transition state is higher than the density of states for the tight transition state, resulting in re-dissociation of the initial complex which is faster than the intramolecular S_N2 reaction.

In solution, the reactant anion is surrounded by many solvent molecules. The localized charge on the nucleophile results in an especially favorable interaction with solvent molecules causing the reactant to be lower in energy in solution compared to the gas-phase analogues. The charge on the complexes represented by the first and second wells in Figure 1b is delocalized over the cluster and as such the complex is significantly less stabilized by interactions with the solvent. Similarly, the transition state is not significantly stabilized by interaction with the solvent due to charge delocalization. The result of greater stabilization of the nucleophile (and product anions) by the solvent, compared with the stabilization of the complexes in the entrance and exit channels as well as the transition state, is the apparent disappearance, in solution, of the features represented by the two intermediate complexes.

There has been much work on the reaction of Cl^- with CH_3-Br. One reason that it is so widely studied is that the experimental results are not well reproduced by statistical theories, indicating that this reaction is nonstatistical.[9−14] Statistical behavior arises when the entrance channel complex has a sufficiently long lifetime to allow for redistribution of its internal energy among all the available internal modes of the complex (intramolecular vibrational energy redistribution or IVR). In order for the complex to live long enough for sufficient IVR to occur, it must either be very large or reside in a deep energy well. The complex initially formed between Cl^- and CH_3Br has few degrees of freedom and is quite weakly bound so that its lifetime prior to reaction is quite short. As well, due to the weak binding, the new vibrational modes associated with the binding of Cl^- to the alkyl halide are poorly coupled to other vibrational modes of the complex[12,14] resulting in poor IVR. Statistical theories, therefore, overestimate the rate constant.[14,15] Conversely, S_N2 reaction rates are well reproduced by statistical theories if the complex in the entrance channel resides in a deep energy well. This may occur with the substitution of a hydrogen with a CN group on the alkyl halide[16] or, if there are larger molecules involved, as with the substitution with a benzyl group,[17] or a large alkyl group.

The HPMS solvation results of halides with acetonitrile, an aprotic solvent, and water, a protic solvent, by both Kebarle and co-workers[18,19] and Hiraoka et al.[20] showed that as the ionic size of the halide increased, from F^- to I^-, the binding energy of the complexes decreased. The complexes that were formed by both Yamdagni and Kebarle[18,19] and Hiraoka et al.[20] that contained only one acetonitrile molecule are complexes of the first well for the potential energy surface for the S_N2 reaction shown in eq 1, where X^- is the halide ion and Y is the cyano group. A handful of other groups have experimentally determined the enthalpy and entropy of clustering reactions of Cl^- onto acetonitrile.[21−23]

The present study is focused on S_N2 reactions of a slightly different nature, as seen in eq 5

$$X^- + R\text{-}CHYCN \rightleftharpoons Y^- + R{-}CHXCN \quad (5)$$

where X and Y are Cl, Br, or I, and R is H, CH_3, or CH_3CH_2. The results of clustering reactions of halide ion and some unsubstituted nitriles are also presented. The identity reaction of eq 5 where $X = Y = Cl^-$ has been studied by Brauman and co-workers[24] both experimentally and computationally. The experiments were carried out using FT-ICR to obtain both the rates of reactions and to determine the binding energy of the complex. The ΔS values were obtained from statistical thermodynamics approximations. They concluded that the complex was bound by purely electrostatic interactions. Contrary to these observations, computational studies by Pagliai et al.[25] concluded that a hydrogen bond between the incoming chloride and the acidic hydrogen on the carbon α to the cyano group was important to the binding. The rates of this reaction have also

been studied by Depuy et al.[26] using a flowing afterglow (FA) apparatus and were found to be in excellent agreement with the experimental results of Brauman and co-workers.[24]

In the present work, the potential energy surfaces for the S_N2 reactions between halide ions and halonitriles were probed using both experimental and computational techniques. Electronic structure calculations involving modest basis sets were used to obtain thermochemical data for stationary points where measurements were not possible.

2. Methods

2.1. Experimental Details. All experiments were carried out in the gas phase with a home-built high-pressure mass spectrometer operating in negative ion mode. The mass analysis was done using a VG Instruments MM 8-80 magnetic sector mass spectrometer. The instrument, constructed at the University of Waterloo, has been described in detail previously.[27]

Gas mixtures were prepared in a 5 L stainless steel reservoir. Methane was used as the inert high-pressure bath gas at a pressure of 800−1000 Torr. The halide ions were generated using trace amounts of CCl_4 for Cl^-, $CHBr_3$ for Br^-, and CH_3I for I^-. The nitriles were added in varying amounts, from 0.1 to 40 Torr, depending on the temperature and binding energy of the complex. All materials were commercial products used without purification. The gas mixture flowed into the ion source at pressures of 5−8 Torr. Ionization was accomplished by 500 μs pulses of 2 keV electrons directed onto a 200 μm aperture in the ion source. A PC-based multichannel scalar (MCS) signal acquisition system configured between 5 and 200 μs dwell time per channel over 250−500 channels was used to monitor the reactions. The results of 1000−3000 electron gun beam pulses were accumulated to generate time intensity profiles of mass selected ions.

Temperature was measured using an iron/constantin thermocouple inserted into a hole in the source block. The temperature is expected to be accurate to ±1 K.

2.2. Determination of Binding Energies. To determine the binding energetics of the halide/neutral complexes, temperature-dependent equilibrium measurements were made for the association reaction in eq 2. An example of ion intensity profiles as a function of time after ionization can be seen in Figure 2a. The corresponding normalized time-intensity profiles are given in Figure 2b, which demonstrate that a steady-state ratio of Br− and Br−...[$CH_3CHClCN$] intensities is established. The intensities of these two ions, I_{X^-} and $I_{X^-\cdots RY}$ respectively, are then used to calculate a dimensionless equilibrium constant using eq 6,

$$K_{eq} = \frac{I_{X^-\cdots RY}}{I_{X^-}} \frac{P^o}{P_{RY}} \tag{6}$$

where P_{RY} is the partial pressure (in atm) of the neutral nitrile in the ion source and P^o is equal to the standard pressure (1 atm). The Gibbs' free energy change is related to the equilibrium constant by eq 7, and to the entropy and enthapy of the reaction by eq 8.

$$\Delta G^o = -RT \ln(K_{eq}) \tag{7}$$

$$\Delta G^o = -\Delta H^o - T\Delta S^o \tag{8}$$

Equating eqs 7 and 8 and dividing by RT yields the van't Hoff equation (eq 9),

$$\ln(K_{eq}) = -\frac{\Delta H^o}{RT} + \frac{\Delta S^o}{R} \tag{9}$$

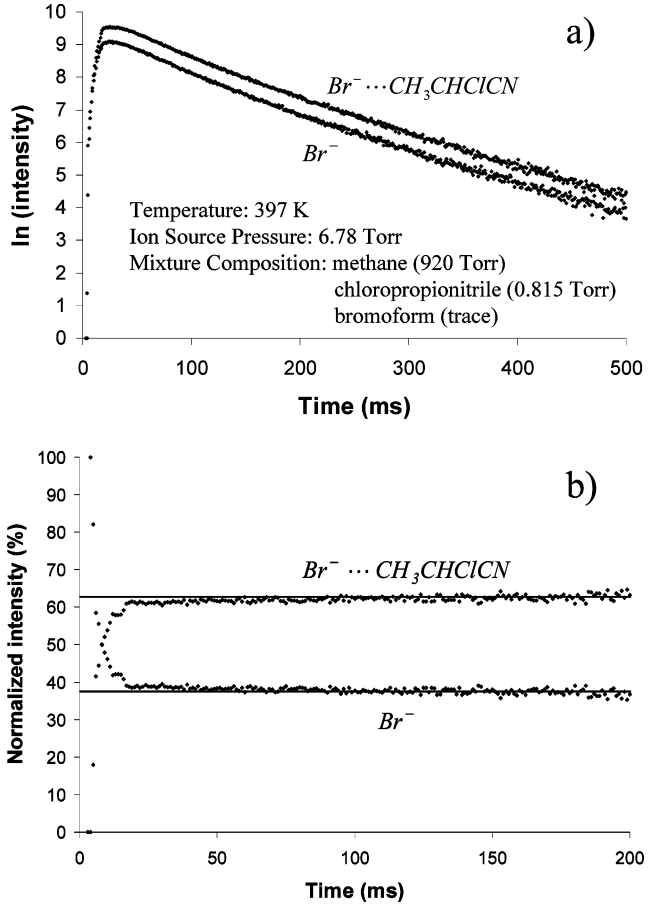

Figure 2. (a) Time−intensity profiles for bromide and its complex with 2-chloropropionitrile and (b) the normalized time−intensity profile. The experimental conditions are given in the figure.

By plotting $\ln(K_{eq})$ versus $1/T$ (van't Hoff plot), one can obtain the enthalpy change, $\Delta H°$, and the entropy change, $\Delta S°$, for the reaction from the slope and intercept, respectively.

2.3. Determination of Central Energy Barriers. The method used to determine the central energy barrier height is similar to that used by Caldwell et al.[28] The rate of reaction for eq 1 can be determined by following the intensity change of the anionic nucleophile as a function of time, as expressed by the rate equation in eq 10,

$$-\frac{dI_{X^-}}{dt} = k^{(2)} I_{X^-}[RY] \tag{10}$$

where $k^{(2)}$ is the second-order rate constant for the reaction. This method eliminates complicating effects due to the rate of diffusion of ions to the ion source walls. Rearranging and integrating the rate equation for the reaction yields eq 11,

$$-\ln \frac{I_{X^-}}{(I_{X^-})_o} = k^{(2)}[RY]t = k't \tag{11}$$

where $(I_{X^-})_o$ is the initial intensity of reactant ion which is unity due to normalization of the data. A plot of $-\ln I_{X^-}$ versus t yields a slope of $k^{(2)}[RY]$, which is the pseudo-first-order rate constant, k', for the reaction. The slope of a plot of k' versus [RY] will yield the second-order rate constant for the S_N2 reaction. According to the Arrhenius equation (eq 12),

$$\ln k^{(2)} = \ln A - \frac{E_a}{RT} \tag{12}$$

a plot of $\ln(k^{(2)})$ vs $1/T$ yields the activation energy from the slope. The enthalpy of activation, $\Delta H^{\ddagger}$, then, is determined from the activation energy, E_a, using eq 13.

$$\Delta H^{\ddagger} = E_a - 2RT \tag{13}$$

The entropy of activation can be determined from the intercept of the Arrenhius plot, A, using eq 14, which is derived from the thermodynamic formulation of transition state theory.

$$\Delta S^{\ddagger} = R\left[\ln\left(\frac{Ah}{k_B T}\right) - 2\right] \tag{14}$$

2.4. Computational Methods. All computational work was done using the Gaussian 98[29] suite of programs. The vibrational frequencies were determined using B3LYP/6-311+G** calculations on optimized geometries from the same level of theory. These geometries were also used to obtain the electronic energies from single-point calculations at the MP2/6-311++G** level of theory. The calculated thermochemical data reported as MP2/6-311++G**//B3LYP/6-311+G** were the MP2 electronic energy combined with the zero-point and thermal contributions derived from the B3LYP calculations. The Stuttgart RLC ECP basis set was used for all iodine-containing species.

3. Results and Discussion

The height of the central barrier plays the decisive role in the reaction rate for exothermic S_N2 reactions. Consequently, in the determination of the entrance channel binding energy, the height of the central barrier with respect to the energy of the reactants is important in determining if the clustering reaction will actually be observed. If the central barrier lies far below the energy of the reactants, the S_N2 reaction is so fast that it would be difficult to observe the entrance channel cluster ions in the present experiments. In these cases the system passes nearly quantitatively over the central barrier to the exit channel forming products. If the barrier lies significantly above the energy of the reactants, then no S_N2 reaction will be observed but the binding energy of the halide to the neutral alkylhalonitrile may be determined.

3.1. Binding Energies. *3.1.1. Halide/Nitrile Binding.* The van't Hoff plots for the clustering of Cl^- onto acetonitrile, propionitrile and butyronitrile are shown in Figure 3. The van't Hoff plots are all linear, which indicates that there is very little or no change in ion structure over the experimental temperature range. The enthalpy and entropy changes for these clustering reactions are also given in Figure 3 and are tabulated with the thermochemical data, Table 1. The terms "well 1" and "well 2" refer to the complexes in the entrance and exit channels for the gas-phase S_N2 reaction as shown in Figure 1b.

The binding energy of Cl^- onto acetonitrile is 60.4 kJ mol^{-1}. A moderate increase is observed for Cl^- onto propionitrile, 63.4 kJ mol^{-1}, but there is a substantially larger increase in binding energy for Cl^- onto butyronitrile, 71.2 kJ mol^{-1}. For hydrogen bonding it would be expected that the binding energy should increase as the acidity of the neutral substrate increases due to the increased ability of the neutral to accommodate some of the negative charge from the halide and result in partial proton transfer. However, experiments show that acetonitrile is slightly more acidic than propionitrile[30] (by 9.0 kJ mol^{-1}) yet propionitrile binds more strongly to Cl^- by 3.0 kJ mol^{-1} relative to acetonitrile. Ab initio calculations support both of these experimental findings (see Tables 1 and 2). To understand the larger binding energy of chloride to propionitrile, one must obviously consider more than just the acidity of the neutral. The structures of the complexes might also contribute to this understanding. Chloride can be considered to be bound to acetonitrile via a hydrogen bond (Figure 4). If the binding in this complex was purely an ion−dipole interaction, the chloride would be oriented along the dipole moment of acetonitrile. The C−H bond distance in acetonitrile increases by 0.015 Å when complexed with chloride, indicating appreciable hydrogen bonding. In propionitrile, the C−H bond on C2 only increases by 0.006 Å, compared with neutral propionitrile, which might indicate a weaker hydrogen bond than in the Cl^-/acetonitrile complex. However, the structure of the Cl^-/propionitrile complex is such that Cl^- is also aligned more closely with the dipole of propionitrile. Propionitrile also has a larger polarizability than acetonitrile due to methyl substitution, which may also contribute to more ion-induced dipole character in the binding of this cluster. It is thus the combination of both hydrogen bonding and ion−dipole interactions that is responsible for the stronger binding of the Cl^-/propionitrile complex. Calculations predict butyronitrile to be more acidic than acetonitrile by 6 kJ mol^{-1} (Table 2). The binding of chloride to butyronitrile is more favorable by 13.4 kJ mol^{-1} relative to acetonitrile. As evidenced by the structure of the Cl^-/butyronitrile complex in Figure 4, the interaction is not just hydrogen bonding at C2. Cl^- is aligned more closely with the dipole of butyronitrile, again accounting for some of the increased binding. Also, the polarizability of butyronitile is larger, increasing the ion-induced dipole interaction.

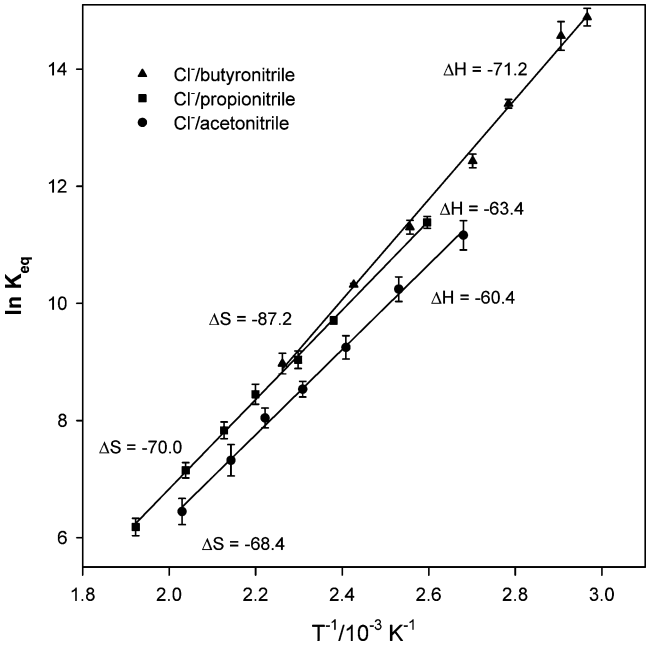

Figure 3. Van't Hoff plots for the clustering of chloride with acetonitrile, propionitrile, and butyronitrile (see legend). Enthalpies and entropies are in kJ mol^{-1} and J K^{-1} mol^{-1}, respectively.

3.1.2. Halide/Halonitrile Binding. Substitution of hydrogen by chlorine and bromine in acetonitrile results in an increased binding of chloride by 21.6 and 22.3 (calculated) kJ mol^{-1}, respectively. This is expected due to the large increase in acidity of the substituted acetonitriles (Table 2). The relationship between the chloride affinity and the calculated acidites of acetonitrile and the substituted nitriles is shown in Figure 5. The binding of chloride to acetonitrile and the substituted nitriles is similar, in that binding is mainly hydrogen bonding (Figure 4). The shortening of the Cl^-- -H bond distances as the substituted acetonitrile becomes more acidic reflects the stronger

TABLE 1: Summary of Experimental and Calculated Thermochemistry[a,b] for Gas-Phase S_N2 Reactions

		entrance channel well		transition state		exit channel well			
X−	nitrile	ΔH^o_1	ΔS^o_1	$\Delta H^‡$	$\Delta S^‡$	ΔH^o_2	ΔS^o_2	$\Delta_{rxn}H^o$	$\Delta_{rxn}S^o$
Cl−	CH_3CN	−60.4 (−59.2)	−68.4 (−81)	(151.2)	(−83)	(−32.4)	(−81)	(130.1)	(36)
Cl−	CH_3CH_2CN	−63.4 (−64.6)	−70.0 (−79)	(159.1)	(−80)	(−36.7)	(−70)	(117.3)	(34)
Cl−	$CH_3CH_2CH_2CN$	−71.2(−72.6)	−87.2(−83)	(150.8)	(−79)	(−38.8)	(−71)	(114.9)	(34)
Cl−	CH_2ClCN	−82.0 (−81.4)	−91.2 (−86)	(−2.8)	(−103)	*c*	*c*	*c*	*c*
Cl−	$CH_3CHClCN$	−84.1 (−86.1)	−86.5 (−86)	(14.9)	(−100)	*c*	*c*	*c*	*c*
Cl−	CH_2BrCN	(−82.7)	(−87)	−18.5 (−25.5)	−88.6 (−103)	−70.7 (−72.0)	−82.0 (−83)	(−39.8)	(−2)
Cl−	$CH_3CHBrCN$	(−87.4)	(−86)	−14.4 (−9.3)	−90.1 (−100)	−76.0 (−77.1)	−83.3 (−84)	(−42.9)	(−2)
Cl−	CH_2ICN	(−78.5)	(−87)	(−23.3)	(−103)	−62.2 (−66.0)	−74.9 (−81)	(−43.9)	(−16)
Cl−	CH_3CHICN	(−83.7)	(−87)	(−5.4)	(−101)	−63.8 (−72.3)	−78.8 (−81.2)	(−47.9)	(−4)
Br−	CH_3CN	−51.8 (−51)	−60.2 (−77)			(−33.1)	(−84)	(171.0)	(37)
Br−	CH_3CH_2CN	−59.4 (−56.6)	−74.7 (−73)			(−38.2)	(−73)	(160.9)	(36)
Br−	CH_2BrCN	−74.5 (−73.5)	−86.2 (−84)	(1.9)	(−101)	*c*	*c*	*c*	*c*
I−	CH_3CN	−48.1 (−47.5)	−64.7 (−77)						
I−	CH_3CH_2CN	−52.2 (−54.1)	−71.2 (−70)						
I−	CH_2BrCN	−69.0	−94.6						

[a] Estimated accuracy of the experimental ΔH^o and ΔS^o are 4 kJ mol^{-1} and 10 J K^{-1} mol^{-1}, respectively. The estimated accuracy of the experimental $\Delta H^‡$ and $\Delta S^‡$ are expected to be similar. [b] Values in parentheses are the computed values. All enthalpy values are in kJ mol^{-1} and entropy values are in J K^{-1} mol^{-1}. [c] Symmetric reaction, so well depths are the same and $\Delta_{rxn}H^o$ and $\Delta_{rxn}S^o$ are 0.

TABLE 2: Comparison of Acidity[a] of Some Nitriles

nitrile	B3LYP/6-311+G**/ kJ mol^{-1}	experiment[b]/ kJ mol^{-1}
acetonitrile	1554	1560
propionitrile	1564	1569
butyronitrile	1548	
chloroacetonitrile	1494	
bromoacetonitrile	1486	
chloropropionitrile	1504	
bromopropionitrile	1496	

[a] Values reported are enthalpies for the general reaction, $MH \rightarrow M^- + H^+$. [b] From reference 30.

binding. Note also that the C−H bond distance is 0.008 Å longer in all of the halogen-substituted acetonitrile/Cl^- complexes than in the acetonitrile/Cl^- complex, reflecting the larger acidity of the substituted acetonitriles. Substitution of hydrogen by chlorine and bromine on propionitrile results in the same effect on the binding of chloride as in the acetonitiles. In Figure 5, the linear relationship mimics that of the acetonitrile/substituted acetonitrile trend, simply offset to higher binding energy due to the stronger binding of chloride to the propionitriles. As found for propionitrile/Cl^- binding, there is some degree of electrostatic binding due to increased ion−dipole interactions.

Calculations predict that Cl^- binding to CH_2ICN and CH_3CHICN is weaker than both the chloro and bromo analogues. This prediction is, at first, completely counterintuitive due to the large degree of ion−dipole binding that iodo substitution on the nitriles should enhance and, then, result in stronger binding. Glukhovstev et al.[31] predicted a similar trend when studying halide/methyl halide complexes, also using an ECP basis for iodine. For Cl^-, Br^-, and I^-, methyl iodide was predicted to be slightly less strongly bound than methyl bromide. In the absence of an explanation and supportive experimental values to justify these predictions, we suggest that the use of ECP on these complexes may underestimate the binding when there is a covalent bond including the atom for which the ECP is used. Note that the calculations of iodide to the nitriles agree well with experiment but this is due to the electrostatic nature of the binding in these cases. Very similar results are obtained using the LANL2DZ+ECP basis set for iodine.

The binding of bromide and iodide to the nitriles and substituted nitriles follows the same trend as that observed for chlorine binding for the same reasons as those discussed above. Structures for the ion−molecule complexes of bromide and iodide to acetonitrile, propionitrile, chloroacetonitrile, chloropropionitrile, and bromoacetonitrile are shown in Figures 6 and 7.

3.1.3. Trend in Binding Different Halides. An interesting trend that deserves discussion is the binding of a particular neutral to each of the halides. For example, the binding energies of Cl^-, Br^-, or I^- to acetonitrile decrease over the series, 60.4, 51.8, and 48.1 kJ mol^{-1}, respectively. Literature values range from 56.1 to 70.3 kJ mol^{-1} for Cl^-, 50.6 to 59.8 kJ mol^{-1} for Br^-, and 46.0 to 50.0 for I^-.[32] The present experimental values are in good agreement with the literature values and are in excellent agreement with the calculated values in Table 1. The binding energy decreases over this series due to the decreasing basicity of the halide, as expected for complexes bound with a substantial

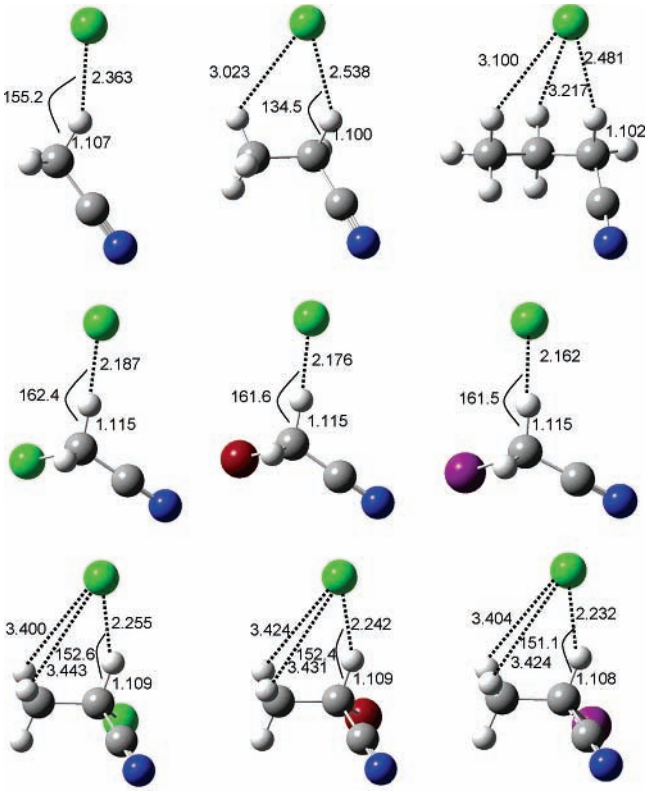

Figure 4. B3LYP/6-311+G**-calculated structures of the complexes of chloride with the various nitriles and halogen-substituted nitriles studied in this work. Bond lengths are in angstroms, and angles are in degrees.

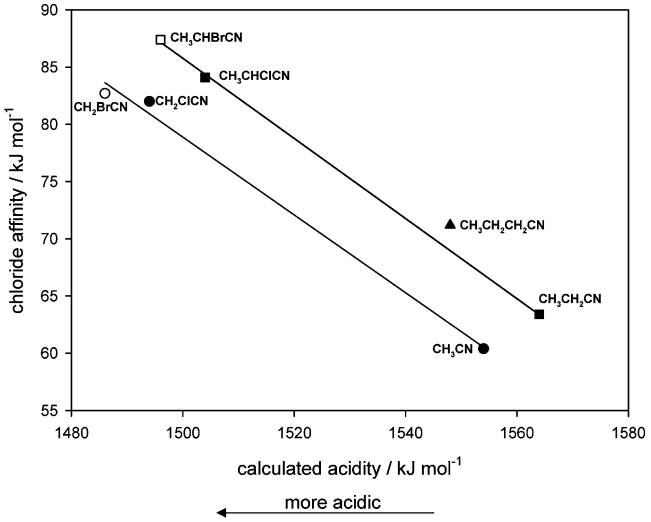

Figure 5. Plot of chloride affinity vs calculated acidity (α to the nitrile group) for various nitriles. The open symbols denote calculated chloride affinities, and the solid symbols denote experimental chloride affinities.

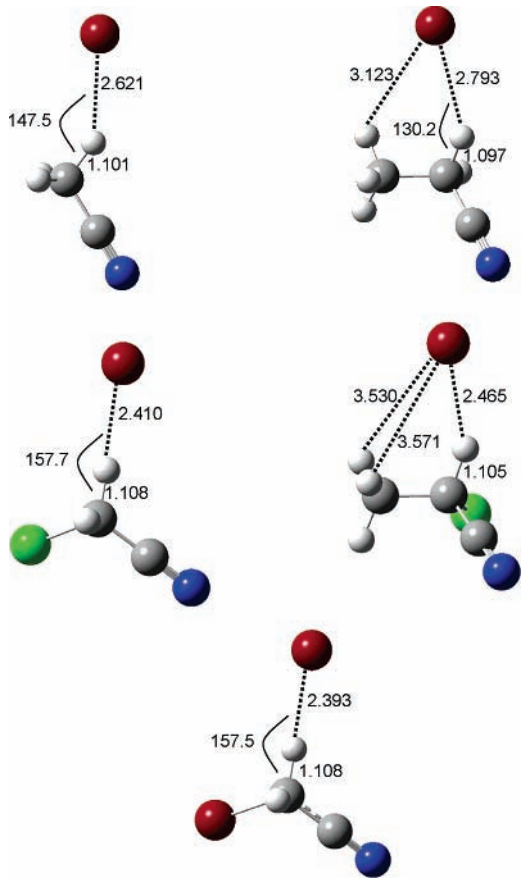

Figure 6. B3LYP/6-311+G**-calculated bromide/nitrile complexes studied in this work. Bond lengths are in angstroms, and angles are in degrees.

degree of hydrogen bonding, and the trend can be seen in Figure 8. This trend of decreasing binding energy with decreasing basicity is also observed for the complexes involving propionitrile and butyronitrile, as well as for the more strongly bound chloroacetonitrile and 2-chloropropionitrile complexes. It is interesting to examine the computed structures for the complexes. Previously, HF/3-21G+p calculations predicted that F^- was bound to acetonitrile via a hydrogen bond, with a structure similar to that for the Cl^-/acetonitrile complex in Figure 4. However in the same study, Cl^-, Br^-, and I^- were found to be

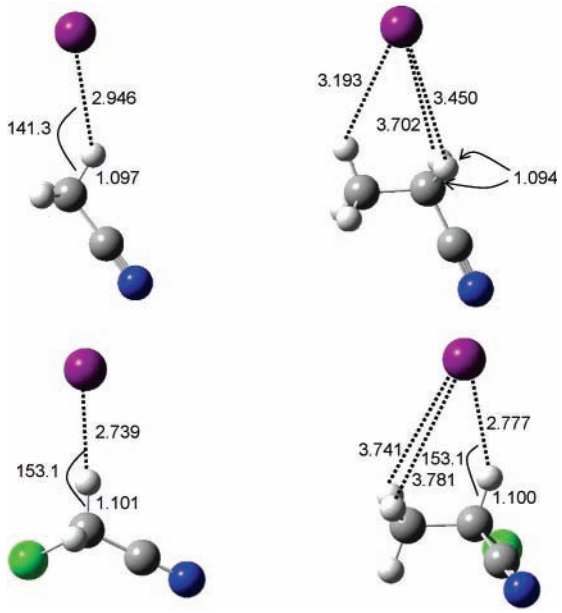

Figure 7. B3LYP/6-311+G**-calculated iodide/nitrile complexes studied in this work. Bond lengths are in angstroms, and angles are in degrees.

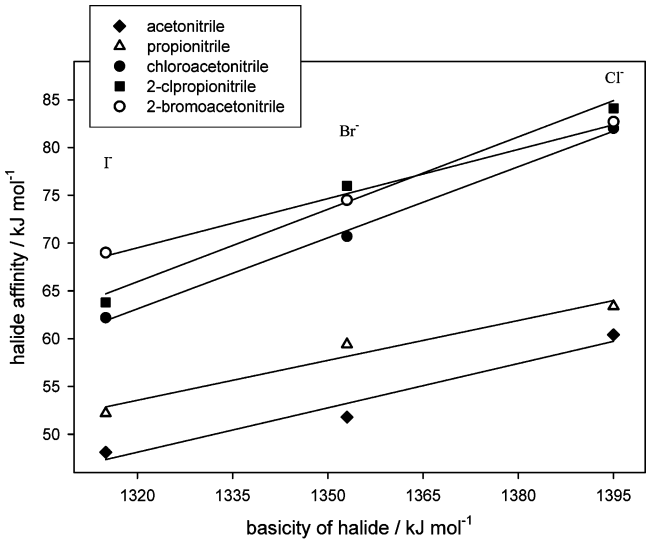

Figure 8. Plot of halide affinity versus the basicity of the halide for the various nitriles and substituted nitriles (see legend). The lines are least-squares fits to the data and are intended to guide the eye.

oriented along the dipole of acetonitrile, leading to the conclusion that the interaction was completely electrostatic. The present calculations are not in agreement and show that, like F^-, the heavier halides are bound via a hydrogen bond to acetonitrile (Figures 4, 6, and 7). In fact the ion−dipole structure at the present level of theory is a transition state. The motion associated with the imaginary frequency is rotation of acetonitrile leading to the hydrogen-bonded structure. The C−H bond length in the halide/acetonitrile complexes does decrease for the larger halides reflecting a lower degree of hydrogen bonding. The C−H−Y (Y = halide) angle decreases over the same series so that the heavier halides are aligned more closely with the dipole of acetonitrile indicating a slight shift from hydrogen bonding to ion−dipole bonding. This is consistent with the decrease in binding energy for the larger halides because the propensity to "share" their electron density by forming a hydrogen bond is not as strong. The bonding in the halide/acetonitrile complexes can, then, be considered to be a mixture of both hydrogen

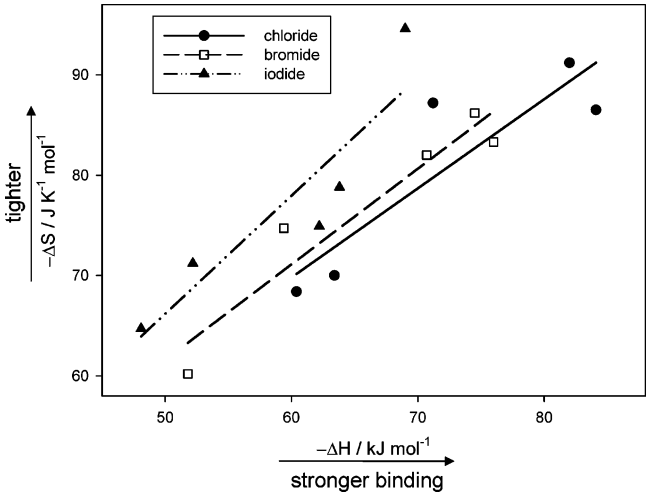

Figure 9. Plot of the negative of the clustering entropy vs the negative of the enthalpy for clustering for the chloride, bromide, and iodide complexes with various nitriles. All values are experimentally determined. The lines are least-squares fits to the data and are intended to guide the eye and show the trends in the data.

bonding and ion−dipole bonding. The effect is most pronounced with the propionitrile series. For both Cl^- and Br^-, the minimum-energy structure is one that has the halide hydrogen bonded to the nitrile, with a slightly elongated C−H bond. The halide is not situated along the dipole of the nitrile. However, the C−H bond distances in the I^-/propionitrile complex are the same as those in neutral propionitrile. Furthermore, the I^-−H bond distances for the most acidic hydrogen atoms (on C2) are quite long, ≥3.4 Å and I^- is oriented directly along the dipole of neutral propionitrile. The bonding in the I^-/propionitrile complex can be considered to be exclusively electrostatic ion−dipole bonding.

3.1.4. Comparison of Enthalpy and Entropy of Binding. It is worthwhile to compare binding enthalpy with the entropy changes for the clustering reactions. In Figure 9 the negative of the entropy change versus the negative of the enthalpy change for binding is plotted. This can be regarded as a comparison of the tightness of the complex versus the strength of binding of the complex. In general, and as expected, stronger binding leads to a greater loss of entropy or a tighter complex. However, the heavier the halide, the weaker the binding (see above), but this weaker binding is accompanied by, *on average*, a complex that is not as loose as expected. The extra tightness of the complexes with the heavier halides may be due to the combination of hydrogen bonding and ion−dipole bonding suggested above, which forces the complex to a geometry that favors both types of binding simultaneously.

3.2. S_N2 Central Energy Barriers. Prior to obtaining the time intensity profiles for these kinetics experiments the entire mass range was examined at each temperature and pressure. In no experiment did we observe any significant signal other than the product ion. For example, in the case of the chloride/bromoacetonitrile reaction the only two ions observed in the mass spectrum were chloride and bromide. At the concentrations used, there was absolutely no clustering observed. The first-order disappearance rate of the Cl^- ion as a function of bromopropionitrile concentration is shown in Figure 10a. The corresponding pseudo-first-order rate constants obtained from these plots, $k^{(1)}$, are plotted against concentration as shown in Figure 10b for the same reaction. The slope of $k^{(1)}$ versus concentration yields the second-order constants, $k^{(2)}$, of Cl^- and bromopropionitrile at 474 K. The Arrhenius plots are shown in

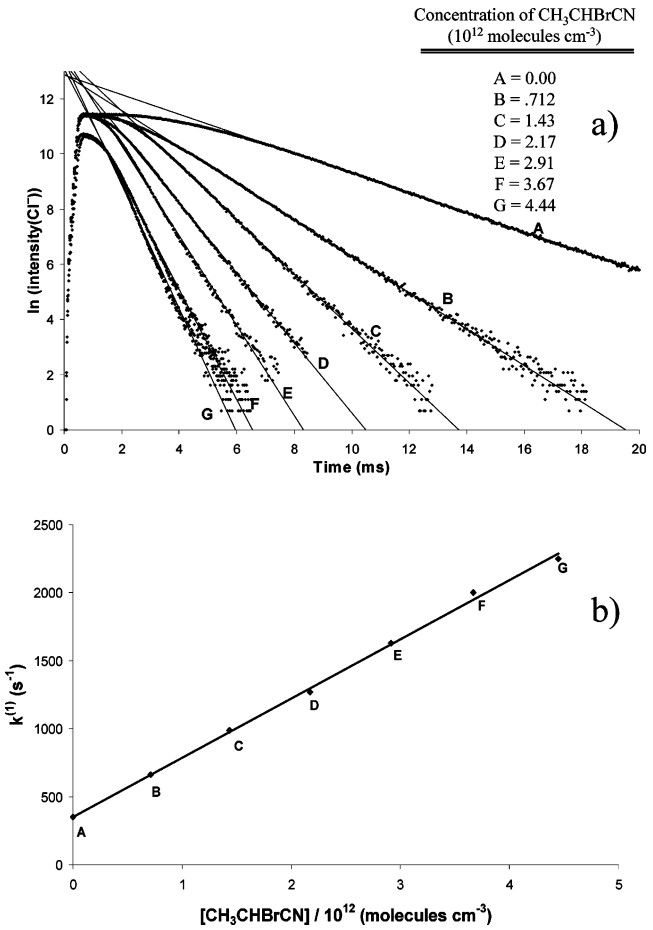

Figure 10. (a) Plot of chloride intensity vs time for the reaction of chloride with 2-bromopropionitrile at various concentrations given in the legend, the slopes of which yield pseudo-first-order rate constants. (b) Plot of the pseudo-first-order rate constants vs concentration, the slope of which yields the second-order rate constant. The concentration of nitriles in these experiments was low enough that no clustering was observed.

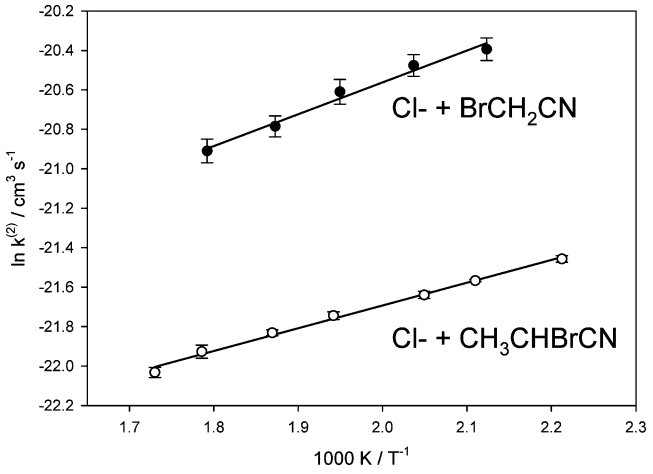

Figure 11. Arrhenius plots for the reactions of chloride with bromoacetonitrile and 2-bromopropionitrile.

Figure 11 and the enthalpy and entropy barriers for the reactions of chloride with bromoacetonitrile and 2-bromopropionitrile obtained from the slopes and intercepts via eqs 13 and 14, respectively, are reported in Table 1. The barrier for the 2-bromopropionitrile reaction is larger than that for the bromoacetonitrile reaction likely due to the added steric effects associated with the reaction upon substitution of a hydrogen for a methyl group. Increased energy barriers for S_N2 reactions

of more highly substituted alkyl bromides have been observed previously. The calculations do predict the proper energy order of these barriers, but the agreement is not quite as satisfactory as that for the thermochemical data for the entrance and exit channel complexes. Experiments yield a difference in barrier heights of 4.1 kJ mol^{-1}, and calculations predict a difference of 16.2 kJ mol^{-1}.

Based on the calculations reported here, it is expected that the chloride substitution reaction of bromoacetonitrile would be a kinetically more favorable process than the identity substitution reaction between chloride and chloracetonitrile. This is in agreement with the ordering of the measured rate constants for the Cl^-/chloroacetonitrile (3.2×10^{-10} cm^3 s^{-1})[26] and Cl^-/bromoacetonitrile (13×10^{-10} cm^3 s^{-1}) reaction.

The S_N2 reaction of Cl^- and CH_3Br has been of particular interest to many groups. The central barrier height for this reaction was determined to be -7.5 kJ mol^{-1} with respect to the reactants,[23] 6.9 kJ mol^{-1} higher than the barrier for the reaction of Cl^- and CH_2BrCN. The decrease in the barrier upon nitrile substitution is expected due to its ability to stabilize the negative charge shared by the chloride and bromide in the transition state structure.

4. Conclusions

The stationary points on the potential energy surfaces for various gas-phase S_N2 reactions have been determined using a combination of pulsed ionization high-pressure mass spectrometry and electronic structure calculations. MP2/6-311++G**//B3LYP/6-311+G** calculations are shown to provide very good agreement with the experimentally determined values, providing confidence for the use of this computational method to predict values that are too difficult or impossible to obtain with the present experimental set up.

The trends in the binding energies of the halides onto the nitriles and substituted nitriles cannot be rationalized in terms of simply hydrogen bonding or ion−dipole bonding but a mixture of the two.

Acknowledgment. TBM thanks the Natural Sciences and Engineering Research Council of Canada for continued support as well as support from the American Chemical Society Petroleum Research Fund.

References and Notes

(1) For the latest reviews see: (a) Laerdahl, J. K.; Uggerud, E. *Int. J. Mass Spectrom.* **2002**, *214*, 277. (b) Hase, W. L. S_N2 Reactions and their Double-Well Potentials. *The Encyclopedia of Mass Spectrometry*; 2005; Vol. 4.

(2) Isaacs, N. S. *Physical Organic Chemistry*, 2nd ed.; Longman Group Limited: Essex, U.K., 1995.

(3) Ingold, C. K. *Structure and Mechanism in Physical Organic Chemistry*, 2nd ed.: Cornell University Press: Ithaca, NY, 1969.

(4) Bohme, D. K.; Young, L. B. *J. Am. Chem. Soc.* **1970**, *92*, 7354.

(5) Bohme, D. K.; Mackay, G. L.; Payzant, J. D. *J. Am. Chem. Soc.* **1974**, *96*, 4027.

(6) Brauman, J. I.; Olmstead, W. N.; Lieder, C. A. *J. Am. Chem. Soc.* **1974**, *96*, 4030.

(7) Olmstead, W. N.; Brauman, J. I. *J. Am. Chem. Soc.* **1977**, *99*, 4219.

(8) (a) Dougherty, R. C.; Dalton, J.; Roberts, J. D. *Org. Mass Spectrom.* **1974**, *8*, 77. (b) Dougherty, R. C.; Roberts, J. D. *Org. Mass Spectrom.* **1974**, *8*, 81. (c) Dougherty, R. C. *Org. Mass Spectrom.* **1974**, *8*, 85.

(9) Viggiano, A. A.; Morris, R. A.; Paschkewitz, J. S.; Paulson, J. F. *J. Am. Chem. Soc.* **1992**, *114*, 10477.

(10) Graul, S. T.; Bowers, M. T. *J. Am. Chem. Soc.* **1994**, *116*, 3875.

(11) Wong, H.; Hase, W. *J. Am. Chem. Soc.* **1995**, *117*, 9347.

(12) Tonner, D. S.; McMahon, T. B. *J. Am. Chem. Soc.* **2000** *122*, 8783.

(13) Wang, Y.; Hase, W. L.; Wang, H. *J. Chem. Phys.* **2003**, *118*, 2688.

(14) Wang, W.; Peslherbe, G. H.; Hase, W. L. *J. Am. Chem. Soc.* **1994**, *116*, *6*, 9644.

(15) Craig, S. L.; Brauman, J. I. *Science* **1997**, *276*, 1536.

(16) Viggiano, A. A.; Morris, R. A.; Su, T.; Wladkowski, B. D.; Craig, S. L.; Zhong, M.; Brauman, J. I. *J. Am. Chem. Soc.* **1994**, *116*, 2213.

(17) Wladkowski, B. D.; Wilbur, J. L.; Brauman, J. I. *J. Am. Chem. Soc.* **1994**, *116*, 2471.

(18) Arshadi, M.; Yamdagni, R.; Kebarle, P. *J. Phys. Chem.* **1970**, *74*, 1475.

(19) Yamdagni, R.; Kebarle, P. *J. Am. Chem. Soc.* **1972**, *94*, 2940.

(20) Hiraoka, K.; Mizuse, S.; Yamabe, S. *J. Phys. Chem.* **1988**, *92*, 3943.

(21) Larson, J. W.; McMahon, T. B. *J. Am. Chem. Soc.* **1984**, *106*, 517.

(22) Sieck, L. W. *J. Phys. Chem.* **1985**, *89*, 5552.

(23) Li, C.; Ross, P.; Szulejko, J. E.; McMahon, T. B. *J. Am. Chem. Soc.* **1996**, *118*, 9360.

(24) Wladkowski, B. D.; Lim, K. F.; Allen, W. D.; Brauman, J. I. *J. Am. Soc. Chem.* **1992**, *114*, 9136.

(25) Pagliai, M.; Raugei, S.; Cardini, G.; Schettino, V. *Phys. Chem. Chem. Phys.* **2001**, *3*, 2559.

(26) DePuy, C. H.; Gronert, S.; Mullin, A.; Bierbaum, V. M. *J. Am. Chem. Soc.* **1990**, *112*, 8650.

(27) Szulejko, J. E.; Fisher, J. J.; McMahon, T. B.; Wronka, J. *Int. J. Mass Spectrom. Ion Processes* **1988**, *83*, 147.

(28) Caldwell, G.; Magnera, T. F.; Kebarle, P. *J. Am. Chem. Soc.* **1984**, *106*, 959.

(29) Frisch, M. J.; Trucks, G. W.; Schlegel, H. B.; Scuseria, G. E.; Robb, M. A.; Cheeseman, J. R.; Zakrzewski, V. G.; Montgomery, J. A., Jr.; Stratmann, R. E.; Burant, J. C.; Dapprich, S.; Millam, J. M.; Daniels, A. D.; Kudin, K. N.; Strain, M. C.; Farkas, O.; Tomasi, J.; Barone, V.; Cossi, M.; Cammi, R.; Mennucci, B.; Pomelli, C.; Adamo, C.; Clifford, S.; Ochterski, J.; Petersson, G. A.; Ayala, P. Y.; Cui, Q.; Morokuma, K.; Malick, D. K.; Rabuck, A. D.; Raghavachari, K.; Foresman, J. B.; Cioslowski, J.; Ortiz, J. V.; Stefanov, B. B.; Liu, G.; Liashenko, A.; Piskorz, P.; Komaromi, I.; Gomperts, R.; Martin, R. L.; Fox, D. J.; Keith, T.; Al-Laham, M. A.; Peng, C. Y.; Nanayakkara, A.; Gonzalez, C.; Challacombe, M.; Gill, P. M. W.; Johnson, B. G.; Chen, W.; Wong, M. W.; Andres, J. L.; Head-Gordon, M.; Replogle, E. S.; Pople, J. A. *Gaussian 98*, revision x.x; Gaussian, Inc.: Pittsburgh, PA, 1998.

(30) Bartmess, J. E.; Scott, J. A.; McIver, R. T., Jr. *J. Am. Chem. Soc.* **1979**, *101*, 6047.

(31) Glukhovstev, M. N.; Pross, A.; Radom, L. *J. Am. Chem. Soc.* **1996**, *118*, 6273.

(32) NIST Standard Reference Database 69, March 2003 Release (http://webbook.nist.gov).